Orientation measurements during drawing of polypropylene by fluorescence polarization microscopy

F. Pinaud*, J. P. Jarry*, Ph. Sergot and L. Monnerie
Laboratoire P.C.S.M., Ecole Supérieure de Physique et de Chimie de Paris, 10, rue Vauquelin, 75231 Paris Cedex 05, France
(*Received 28 May 1981; revised 2 November 1981*)

Fluorescence polarization microscopy was used to investigate the orientation of the amorphous phase of polypropylene. The data are corrected for light scattering effects. The second and fourth moments of orientation are measured (1) through the necking zone of cold drawn samples, and (2) during stretching at various temperatures. The results show that amorphous orientation depends mainly on the crystalline orientation and morphology. This suggests that the amorphous chains are strongly embedded in the crystalline phase.

Keywords Orientation measurements; polypropylene; drawing, fluorescence polarization microscopy; amorphous phase; light scattering effects

INTRODUCTION

Several studies have been reported in the literature[1-4] on the orientation and morphology of drawn polypropylene. However, the molecular mechanisms occurring during stretching are far from being fully understood. The structure has been investigated only *after* drawing and only at room temperature. The crystalline morphology has been extensively studied by diffraction and scattering techniques, but the orientation of the amorphous phase has been determined indirectly, from birefringence and a few other techniques, by measuring an average orientation and substracting the crystalline component. This procedure suffers from various difficulties which have been discussed in detail[5].

The advantage of the fluorescence polarization technique is twofold. Firstly, the second and fourth moments of the amorphous orientation distribution are obtained directly, since the fluorescent probe molecules are located in the amorphous phase, as shown by Nobbs *et al.*[6] in the case of drawn poly(ethylene terephthalate). Secondly, changes in orientation can be easily monitored during the process of drawing. In the present work, we report the use of fluorescence polarization microscopy to study the amorphous orientation in uniaxially drawn polypropylene. Two kinds of experiments have been performed: (a) longitudinal profiles of orientation have been measured after drawing in the necking zone, with a microscope; (b) changes in orientation have been recorded during stretching. The results are compared with published data on the behaviour of the crystalline phase.

THEORY OF FLUORESCENCE POLARIZATION

Basic theory

The basic theory of fluorescence polarization has been developed by Desper[7], in the ideal case where the following conditions are fulfilled: (a) no rotational motion of the fluorescent probe occurs during the fluorescence lifetime (of the order of 10^{-8} second); (b) the transition moments in both absorption and emission coincide with a molecular axis $\underline{M}$ of the probe (no electronic delocalization); (c) the state of polarization of the excitation and fluorescence lights are not changed by birefringence or scattering.

For uniaxial stretching along the Ox_3-axis (see *Figure 1*), the fluorescence intensities i_{ij} measured with the polarizer along Ox_i and the analyser along Ox_j are given by:

$$i_{33} = k\langle\cos^4\theta\rangle \tag{1a}$$

$$i_{31} = i_{13} = k\langle\cos^2\theta\,\sin^2\theta\rangle/2 \tag{1b}$$

$$i_{11} = 3k\langle\sin^4\theta\rangle/8 \tag{1c}$$

where θ is the angle between the symmetry axis Ox_3 and the molecular axis $\underline{M}$. The brackets denote an ensemble average over all the fluorescent molecules. The second and fourth moments of the orientation distribution can be calculated from the above intensities:

$$\langle\cos^2\theta\rangle = \frac{i_{33}+2i_{31}}{(8/3)i_{11}+4i_{31}+i_{33}} \tag{2a}$$

$$\langle\cos^4\theta\rangle = \frac{i_{33}}{(8/3)i_{11}+4i_{31}+i_{33}} \tag{2b}$$

The temperature dependence of the fluorescence polarization from isotropic polypropylene shows that rotational motion is negligible at temperatures not higher than 80°C. Condition (a) is fulfilled in the experiments of this work. On the contrary, assumptions (b) and (c) are not valid and the effects of light scattering and electronic delocalization are dealt with in the next two sections.

* Present address: Centre de Recherche de Saint-Fons, Rhône-Poulenc, 69190 Saint Fons, France

0032—3861/82/111575-06$03.00

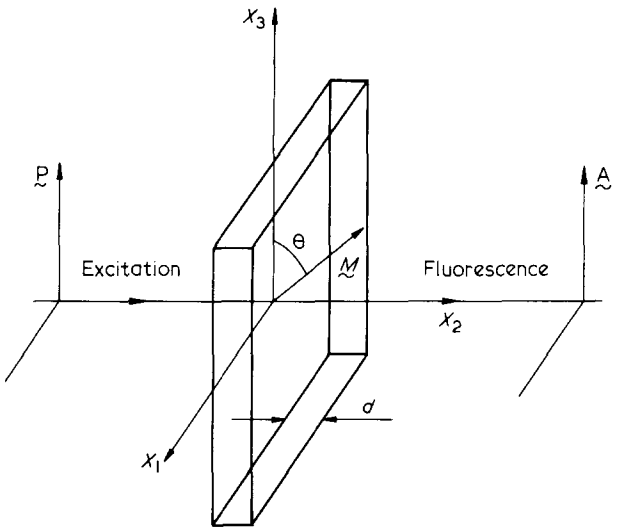

Figure 1 Schematic representation of the fluorescence polarization experiment, P: polarizer; A: analyser; M: transition moment

Light scattering correction

The principle of a method of correction for birefringence, absorption and scattering effects has been given briefly by Nobbs[6]. In the experiments presented in this work, the directions of the polarizer and the analyser coincide with the principal directions of the stress tensor and birefringence can be ignored. In addition, the concentration of fluorescent molecules is very small, and absorption can be safely neglected. Accordingly, we restrict ourselves to a detailed calculation of the scattering correction, in the case where the excitation and fluorescence beams are collinear, as shown in *Figure 1*.

When the impinging light beam, directed along Ox_2 and polarized along Ox_i ($i=1,3$), propagates through a semicrystalline sample, its state of polarization is strongly altered by scattering[8]. Consequently, a fluorescent probe located at depth X within the sample is excited by a partially polarized light, with two components along Ox_i and Ox_j ($i, j=1, 3$).

$$I_{ie}(X)=I_0E_i(X)$$
$$I_{je}(X)=I_0(1-E_i(X)) \tag{3}$$

where:

$$E_i(X)=\exp(-\tau_{ie}X)$$

I_0 is the intensity of the impinging beam and τ_{ie} is the turbidity for the excitation wavelength polarized along Ox_i. Accordingly, the fluorescence light generated at depth X has two components polarized along Ox_i and Ox_j:

$$I_{if}(X)=E_i(X)i_{ii}+(1-E_i(X))i_{ji}$$
$$I_{jf}(X)=E_i(X)i_{ij}+(1-E_i(X))i_{jj}$$

That light travels through $(d-X)$ and the fluorescence light emerging from the sample is given by:

$$I_{ii}(X)=I_{if}F_i(X)+I_{jf}(1-F_j(X))$$
$$I_{ij}(X)=I_{if}(1-F_i(X))+I_{jf}F_j(X)$$

where $F_i(X)=\exp[-\tau_{if}(d-X)]$; τ_{if} is the turbidity for the fluorescence wavelength.

Averaging over the variable X ($0\leqslant X\leqslant d$), the final expressions are obtained for the intensities I_{ij} measured with the polarizer and the analyser directed along Ox_i and Ox_j respectively:

$$I_{ii}=A_ii_{ii}+(B_i+C_i-A_i-D_{ij})i_{ij}+(1-B_j-C_i+D_{ij})i_{jj}$$
$$I_{ii}=(C_i-A_i)i_{ii}+(1-B_i-C_i+A_i+D_{ij})i_{ij}+(B_j-D_{ij})i_{jj} \tag{4}$$

where

$$A_i=(\tau_{if}d-\tau_{ie}d)^{-1}[\exp(-\tau_{ie}d)-\exp(-\tau_{if}d)]$$
$$B_i=(\tau_{if}d)^{-1}[1-\exp(-\tau_{if}d)]$$
$$C_i=(\tau_{ie}d)^{-1}[1-\exp(-\tau_{ie}d)]$$
$$D_{ij}=(\tau_{jf}d-\tau_{ie}d)^{-1}[\exp(-\tau_{ie}d)-\exp(-\tau_{jf}d)]$$

By the use of adequate optical filters, the intensities $I_{ie}(d)$, $I_{je}(d)$, $I_{if}(d)$ and $I_{jf}(d)$, transmitted through the sample for both excitation and fluorescence wavelengths, can be easily measured. The four corresponding turbidities are then calculated using equation (3) with $X=d$. Finally, the intensities i_{ij} of the basic theory (equation (1)) are derived from the measured intensities I_{ij} by use of equations (4).

It is worth noting that the above treatment accounts for the difference $I_{ij}\neq I_{ji}$, in anisotropic materials which is always observed in semicrystalline polymers, whereas the basic theory predicts $i_{ij}=i_{ji}$.

Electronic delocalization correction

As a result of the fluctuations of the electronic distribution, the transition moments in absorption and in emission do not coincide with the molecular axis M. Their directions with respect to M must be defined by two orientation distributions δ_a and δ_e respectively. The main problem when dealing with delocalization is to know whether δ_a and δ_e are identical. Kimura[9] has proposed that the difference between δ_a and δ_e is responsible for the observed asymmetry $I_{ij}\neq I_{ji}$. However, for all the fluorescent probes we have used, the symmetry $I_{ij}=I_{ji}$ is satisfied in drawn amorphous polymers, the scattering for which is weak. It is thus reasonable to assume that δ_a and δ_e are identical and that the asymmetry, observed in semicrystalline polymers only, is due to scattering. The theory, developed earlier[10] for the case $\delta_a=\delta_e$, shows that the second and fourth moments of orientation can be obtained from the knowledge of the intensities i_{ij} (after correcting for scattering) and one measurement of the limit anisotropy r_0* in the isotropic state:

* In an isotropic medium, r_0 is defined as:

$$r_0=\left\langle\frac{3\cos^2\alpha-1}{5}\right\rangle$$

where α is the angle between the two transition moments, due to electronic delocalization. When molecular motions occur during the lifetime, the time-dependent intensities $i_{33}(t)$ and $i_{13}(t)$ can be monitored (decay experiments). Jablonski[11] has shown that r_0 is the limit of the ratio

$$(i_{33}(t)-i_{13}(t))/(i_{33}(t)+2i_{13}(t))$$

when t tends to zero.

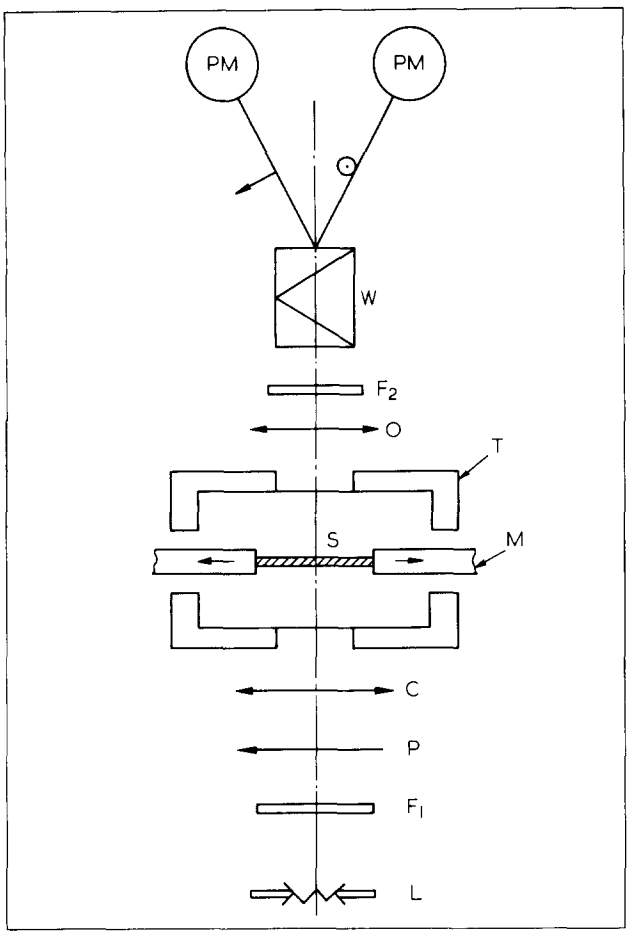

Figure 2 Fluorescence polarization microscope. L, Mercury lamp; F_1, F_2, excitation and fluorescence filters, P, polarizer; C, Condenser; O, Objective; W, Wollaston prism; PM, Phototubes; S, Sample; SM, Stretching machine; T, Thermal enclosure

$$i_{33} = K[1 - 2(5r_0/2)^{1/2} + (5r_0/2) + [6(5t_0/2)^{1/2} - 30r_0/2]\langle\cos^2\theta\rangle + (45r_0/2)\langle\cos^4\theta\rangle]$$

$$i_{11} = K[1 + (5r_0/2)^{1/2} + (55r_0/16) - [3(5r_0/2)^{1/2} + 75r_0/8]\langle\cos^2\theta\rangle + (135r_0/16)\langle\cos^4\theta\rangle]$$

$$i_{13} = K[1 - (5r_0/8)^{1/2} - (5r_0/4) + [3(5r_0/8)^{1/2} + 15r_0/2]\langle\cos^2\theta\rangle - (45r_0/4)\langle\cos^4\theta\rangle]$$

EXPERIMENTAL

Apparatus

A commercial microscope (NACHET, NS 400) has been modified to permit fluorescence polarization measurements during stretching (*Figure 2*). The sample holder was replaced by a small tensile machine, equipped with a stress transducer. The two clamps translate symmetrically, so that the centre of the sample is maintained in the field of the microscope.

The excitation and fluorescence wavelengths are selected by the optical filters F_1 and F_2 respectively. The rotatable polarizer P is oriented alternatively parallel (Ox_3) or perpendicular (Ox_1) to the stretching direction. The state of polarization of the fluorescence light is analysed by a Woolaston prism W, which splits the fluorescence beam into two distinct beams[12]. These beams are polarized along Ox_3 and Ox_1 respectively and are simultaneously measured by the two phototubes. The time required to record a set of intensities (I_{33}, I_{31}, I_{13}, I_{11}) is about 5 seconds.

Materials

The commercially available polymer investigated is a 320000 molecular weight polypropylene (NAPHTACHIMIE, Napryl 61400 AQ), containing 95% isotactic sequences. It crystallizes in the α form (melting point around 160°C). 0.3 mm thick sheets were moulded at 220°C. The shape of the sample has been designed to generate the necking zone under the objective of the microscope, in a reproducible way (*Figure 3*). The degree of crystallinity was estimated to be around 45% from measurements of the average refractive index[13,14]. The helicoidal conformation fraction was about 85%, as determined by infra-red absorption[15,16]. This suggests that a significant number of helicoidal conformations are present in the amorphous phase[17,18].

All-*trans* 1,8-diphenyloctatetraene (DPO) was employed as a fluorescent probe. It was preferred to the more common 1,6-diphenylhexatriene (DPH), because it exhibits a larger gap between absorption and fluorescence wavelengths. This made the choice of optical filters much easier.

Powdered polypropylene was impregnated with a probe in benzene solution. After solvent evaporation, the powder was moulded to give samples having the shape shown in *Figure 3*. The final concentration of the probe ($\simeq 6\times10^{-7}$ mol g^{-1}) was low enough to prevent undesired energy transfer. The anisotropy limit was found to be $r_0 \simeq 0.31$, in agreement with earlier measurements for DPO in polyethylene[19]. This high value of r_0 gave evidence that the probe was satisfactorily dissolved in the polymer matrix. If aggregates had formed, the fluorescence emission would be depolarized by intermolecular energy transfer.

Experimental procedure

To gain knowledge of the orientation profiles after drawing (static experiments) three successive sets of measurements were required:

(1) measurement of the four fluorescence intensities I_{ij}, with the optical filters, F_1 and F_2 centred at $\lambda_e = 365$ nm and $\lambda_f = 520$ nm respectively;

(2) measurement of the two scattering factors $\tau_{ie} \times d$, with F_1 and F_2 centred at λ_e;

(3) measurement of the two scattering factors $\tau_{if} \times d$, with F_1 and F_2 centred at λ_f.

By use of equations (4) and (5), the second and fourth moments ($\langle\cos^2\theta\rangle$ and $\langle\cos^4\theta\rangle$), corrected for electronic

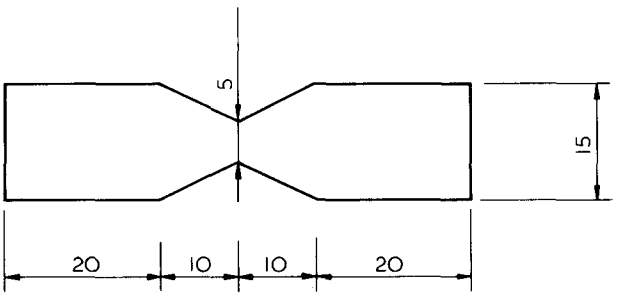

Figure 3 Shape of the sample. Dimensions in millimetres

Table 1 Scattering factors for excitation and fluorescence wavelengths, second and fourth moments calculated for different isotropic samples

$\tau_{3e} \times d$	$\tau_{3f} \times d$	$\langle\cos^2\theta\rangle$ uncorrected	$\langle\cos^4\theta\rangle$ uncorrected	$\langle\cos^2\theta\rangle$ corrected	$\langle\cos^4\theta\rangle$ corrected
0.41	0.25	0.370	0.156	0.333	0.200
0.51	0.29	0.374	0.151	0.334	0.199
0.46	0.27	0.372	0.153	0.335	0.197
0.43	0.25	0.369	0.157	0.329	0.205
0.43	0.25	0.370	0.157	0.330	0.204

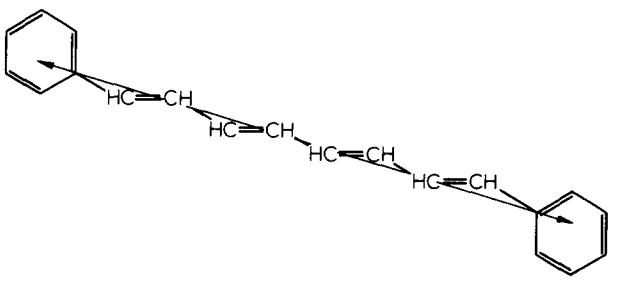

Figure 4 Formula and transition moment (arrow) of 1,8-diphenyl-octatetraene

delocalization and scattering effects, were calculated. The validity of the correction was checked with five unstretched samples. Values of scattering factors ($\tau_e \times d$) and $\tau_f \times d$) are shown in *Table 1*, along with calculated values of $\langle\cos^2\theta\rangle$ and $\langle\cos^4\theta\rangle$. The corrected values approach to within 1% for $\langle\cos^2\theta\rangle$ and 4% for $\langle\cos^4\theta\rangle$ the theoretical values ($\langle\cos^2\theta\rangle = 1/3$ and $\langle\cos^4\theta\rangle = 1/5$).

When changes in orientation were monitored during stretching (dynamic experiment) the three sets of experiments could not be performed simultaneously. For these experiments, the four intensities I_{ij} only were measured and uncorrected values of $\langle\cos^2\theta\rangle$ and $\langle\cos^4\theta\rangle$ were calculated using equation (2).

RESULTS AND DISCUSSION

Behaviour of the probe

The structure and the fluorescence properties of all-*trans* diphenylpolyenes in solution have been extensively studied[20-23]. Although the fluorescence mechanism has not been fully understood, it is generally admitted[22,23] that excitation of the all-*trans* ground state (*Figure 4*) to a planar excited state is followed by a change of configuration, which leads to a twisted form.

The absorption and fluorescence spectra and the value of the fluorescence lifetime of DPO in polypropylene are quite similar to those reported in solution. The fluorescence mechanism is most likely to be the same in polypropylene as in solution. No *cis–trans* photoisomerization can occur in the conditions of the present work.

The use of diphenylpolyenes as probes for orientation or reorientational Brownian motion in a variety of anisotropic materials (nematic liquid crystal[24], membrane lipids[25-27], polymers[19]) has been reported. These studies clearly suggest that these molecules can be considered as rigid rods.

The relation between the orientation of a rigid fluorescent probe and that of the polymer segments has been studied by Nobbs *et al.*[6] by comparing birefringence, i.r. dichroism and fluorescence data. The second moment

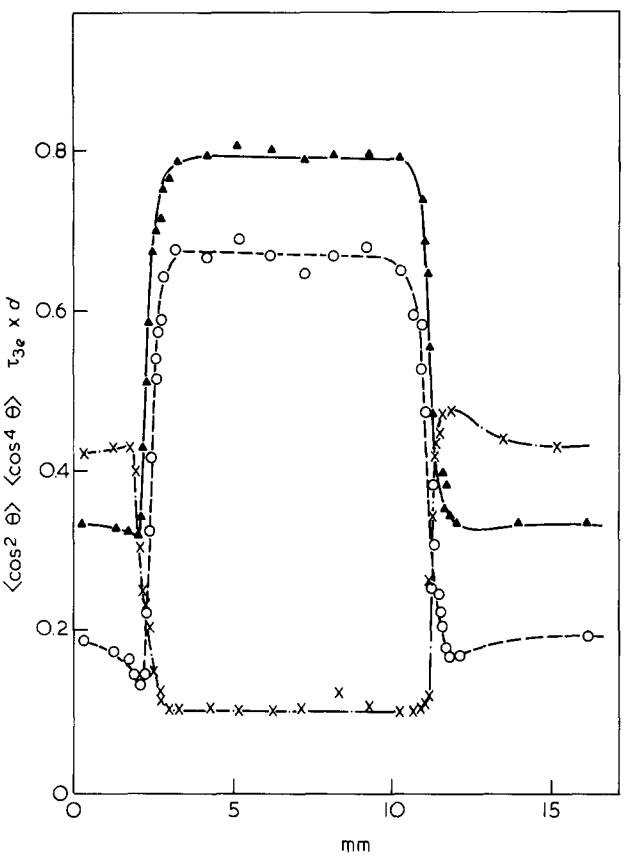

Figure 5 Longitudinal profiles of a sample drawn at room temperature: ▲, $\langle\cos^2\theta\rangle$; ○, $\langle\cos^4\theta\rangle$; X, $\tau_{3e}d$

of the probe is shown to vary linearly with the birefringence of the matrix. It is higher than the estimated second moment of the polymer segments. From a theoretical point of view, a first order treatment[28] of the anisotropic interactions between a guest molecule and the surrounding segments shows that the quantities $\langle\cos^2\theta - 1/3\rangle$ of the guest and of the segments should be proportional, the proportionality constant being unknown.

In conclusion, the second moment of orientation of the fluorescent probe is relevant to that of the polymer segments.

Static experiments

Room temperature profiles of the scattering factor ($\tau_{3e}d$) and the orientation moments are shown in *Figure 5* for a sample drawn at room temperature. Three distinct zones clearly appear: an isotropic zone on both sides of the sample, a uniformly oriented zone in the middle (necked zone) and two narrow transition zones where a sharp change in orientation is observed. As shown in

Table 2 Local thickness, scattering factor and turbidity on three spots of a drawn sample

Zone	d (mm)	$\tau_{3e} \times d$	τ_{3e} (mm^{-1})
Isotropic	0.31	0.49	1.56
Transition	0.10	0.14	1.40
Necked	0.08	0.10	1.12

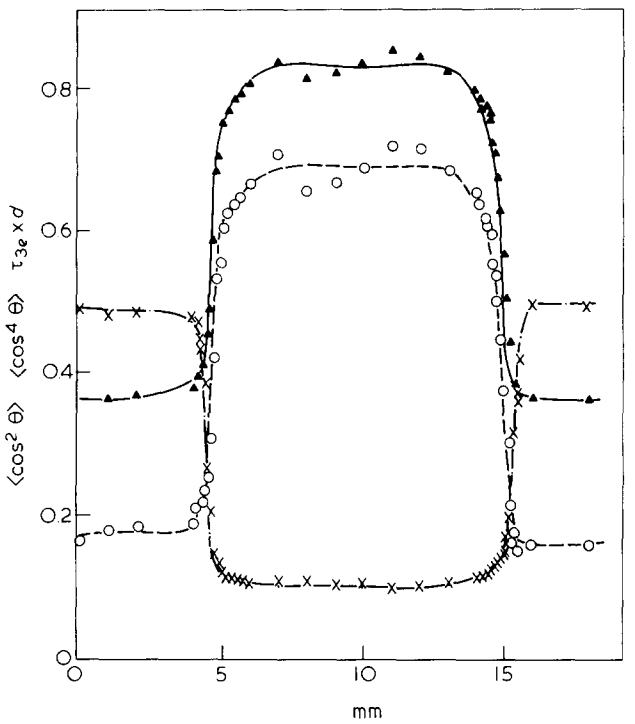

Figure 6 Longitudinal profiles of a sample drawn at 80°C: ▲, $\langle\cos^2\theta\rangle$; ○, $\langle\cos^4\theta\rangle$; X, $\tau_{3e}d$

Table 2, the change in the scattering factor is due mainly to the decrease in the thickness d, whereas the turbidity τ_{3e} varies only slightly. The scattering factor profile reflects the changes in local draw ratio, which is about 6 in the necked zone. These findings are quite consistent with the results published by Peterlin[3], who found that the draw ratio is uniform in the necked zone.

At the beginning of the transition zones, $\langle\cos^2\theta\rangle$ and $\langle\cos^4\theta\rangle$ decrease slightly. By combining birefringence and infra-red measurements, Samuels[1] has already reported similar behaviour, which suggests that the amorphous chains are initially oriented perpendicular to the crystalline lamellae[5]. Accordingly, the rotation of the lamellae toward the stretching axis would induce a negative orientation of the amorphous phase.

The room temperature profiles of a sample drawn at 80°C are shown in *Figure 6*. The transition zones are smoother than in the previous case and the negatively oriented zones are no longer observed. However, it should be pointed out that $\langle\cos^2\theta\rangle$ and $\langle\cos^4\theta\rangle$ have similar values in the necked zone.

In *Figure 7*, $\langle\cos^4\theta\rangle$ is plotted *versus* $\langle\cos^2\theta\rangle$ for the points of the transition and necked zones in *Figures 5* and *6*. Good agreement is obtained with the pseudo-affine model developed by Ward[29]. In fact, the validity of this model has been checked for all static and dynamic experiments. Therefore, the data relative to the fourth moment are omitted in the subsequent section.

Dynamics experiments

The time dependencies of the stress σ, the second moment and the scattering factor are shown in *Figure 8* for stretching at room temperature. Again, the three zones are observed. The isotropic zone corresponds to the elastic part of the stress curve. At long time, the orientation of the amorphous chains levels off, in agreement with earlier studies[4,30,39] which show that the crystalline orientation and morphology remain constant in the necked zone, until the whole sample has necked. The transition zones of $(\tau_{3e} \times d)$ and $\langle\cos^2\theta\rangle$ are not synchronous. The minimum value for the scattering factor is reached sooner than the maximum value of the second moment. This orientation lag is due to the viscoelastic nature of the orientation process, as revealed by relaxation experiments. The tensile machine is stopped when the sample is in the transition zone. It is found (*Figure 9*) that $\langle\cos^2\theta\rangle$ continues to increase significantly.

The effect of crystalline morphology has been investigated by adding a nucleating agent, so that the average diameter of the spherulites is reduced from 20 μm

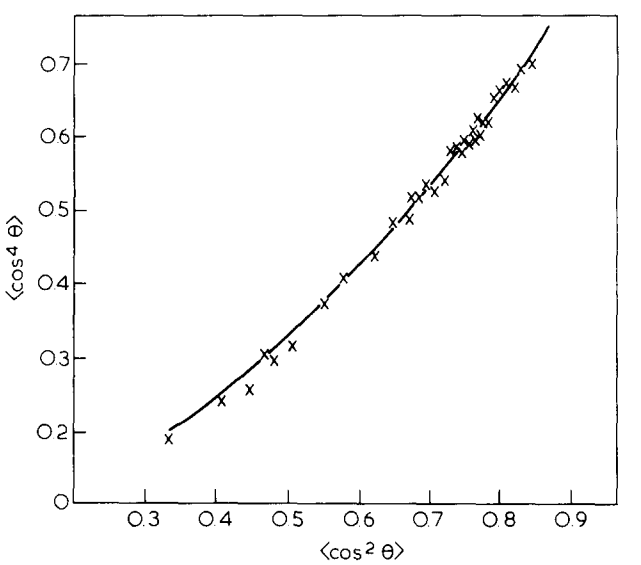

Figure 7 Fourth moment *versus* second moment. X, Experimental; (——), prediction of the pseudo-affine model

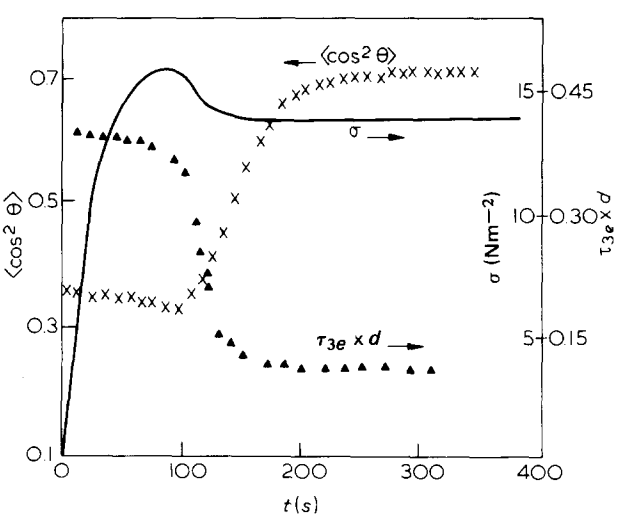

Figure 8 Stress σ, second moment and scattering factor during stretching at room temperature. (——), stress; X, $\langle\cos^2\theta\rangle$; ▲, $\tau_{3e}d$

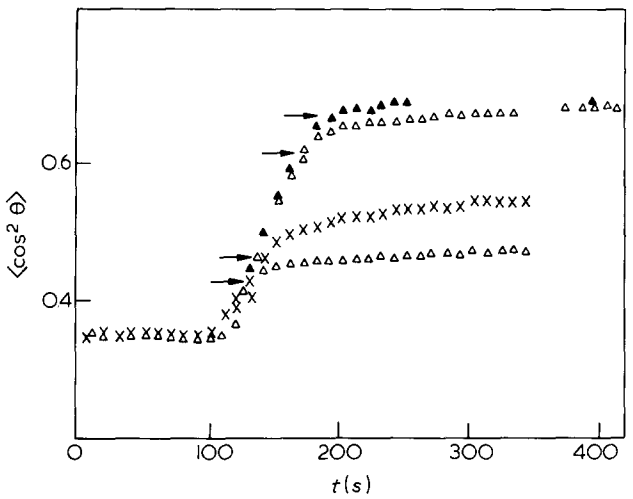

Figure 9 Changes in orientation during relaxation experiments. The arrows mark the times when the strain is halted

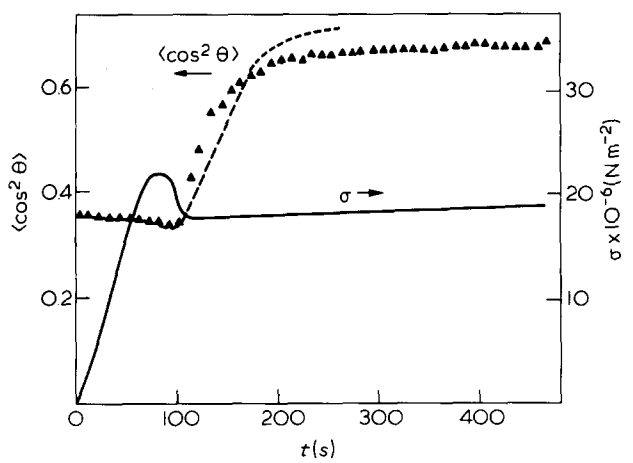

Figure 10 Stress and second moment during stretching of a nucleated sample at room temperature; (——), stress; ▲, $\langle\cos^2\theta\rangle$ of the nucleated sample; (— — — —), $\langle\cos^2\theta\rangle$ for the non-nucleated sample

to 5 μm at room temperature. The nucleated sample crystallizes at higher temperatures when it is cooled after moulding and contains thicker lamellae. As shown in *Figure 10*, the stretching of this sample at room temperature exhibits a sharper transition and a lower maximum of orientation.

CONCLUSION

Fluorescence polarization microscopy provides reliable and valuable information on the amorphous orientation of semicrystalline polymers when the depolarization effects, due mostly to scattering, are properly corrected. This technique is flexible and especially useful when an inhomogeneous distribution of orientation or time dependent phenomena are to be dealt with.

The present work on polypropylene suggests that the amorphous chains are not free to orient or disorient independently of the crystallites. On the contrary, they seem to be strongly embedded in the crystalline phase[36], so that the amorphous orientation is largely determined by crystalline orientation and morphology. This may explain why the pseudo-affine model, which describes the rotation of rigid crystallites, also holds for amorphous orientation.

ACKNOWLEDGEMENTS

This work was supported by a grant from Rhône-Poulenc.

REFERENCES

1 Samuels, R. J. *J. Polym. Sci. A2* 1968, **6**, 1101
2 Samuels, R. J. in 'Solid State of Polymers', (Ed. P. H. Geil), 1974, Marcel Dekker, New York
3 Balta-Calleja, F. J. and Peterlin, A. *J. Macromol. Sci.* 1970, **B4**, 519
4 Balta-Calleja, F. J. and Peterlin, A. *J. Polym. Sci. A2* 1969, **7**, 1275
5 Ward, I. M. 'Structure and Properties of Oriented Polymers' 1975, Appl. Science Publ., London
6 Nobbs, J. M., Bower, D. I., Ward, I. M. and Patterson, D. *Polymer* 1974, **15**, 287
7 Kimura, I. and Desper, C. R. *J. Appl. Phys.* 1967, **38**, 4225
8 Prud'homme, R. E., Bourland, L., Natarajan, R. T. and Stein, R. S. *J. Polym. Sci. Polym. Phys. Edn.* 1974, **12**, 195
9 Kimura, I., Kagiyama, M., Nomura, S. and Kawai, S. *J. Polym. Sci. A2* 1969, **7**, 709
10 Jarry, J. P. and Monnerie, L. *J. Polym. Sci., Polym. Phys. Edn.* 1978, **16**, 443
11 Jablonski, A. *Z. Naturforsch. A* 1961, **16**, 1
12 Jarry, J. P., Sergot, P., Pambrun, C. and Monnerie, L. *J. Phys., Part E* 1978, **11**, 702
13 Shael, G. *J. Appl. Polym. Sci.* 1968, **12**, 903
14 Okajima, S. *J. Appl. Polym. Sci.* 1967, **11**, 1703
15 Abe, K. and Yanagisawa, K. *J. Polym. Sci.* 1959, **36**, 536
16 Quynn, R. G., Riley, J. L. and Young, D. A. *J. Appl. Polym. Sci.* 1959, **2**, 166
17 Peraldo, M. *Gazz. Chim. Ital.* 1959, **89**, 798
18 Painter, P. C., Watzek, M. and Koenig, J. L. *Polymer* 1977, **18**, 1169
19 Nishijima, Y. and Mito, Y. *Rep. Prog. Polym. Phys. Jpn.* 1968, **11**, 425
20 Lo, D. H. and Whitehead, M. A. *Canad. J. Chem.* 1968, **46**, 2041
21 Drenth, W. and Wiebenga, E. H. *Acta Cryst.* 1955, **8**, 755
22 Cehelnik, E. D., Cundall, R. B., Lockwood, J. R. and Palmer, T. F. *Chem. Phys. Lett.* 1974, **27**, 586
23 Cehelnik, E. D., Cundall, R. B., Lockwood, J. R. and Palmer, T. F. *J. Phys. Chem.* 1975, **79**, 1369
24 Cehelnik, E. D., Cundall, R. B., Lockwood, J. R. and Palmer, T. F. *J. Chem. Soc., Faraday Trans.* 1974, **70**, 244
25 Chen, L. A., Dale, R. E., Roth, S. and Brand, L. *J. Biol. Chem.* 1977, **252**, 2163
26 Dale, R. E., Chen, L. A. and Brand, L. *J. Biol. Chem.* 1977, **252**, 7500
27 Heyn, M. P. *F.E.B.S. Lett.* 1979, **100**, 359
28 Jarry, J. P. and Monnerie, L. *Macromolecules* 1979, **12**, 316
29 Ward, I. M. 'Mechanical Properties of Solid State Polymer', 1971, Wiley, Interscience
30 Balta-Calleja, F. J. and Peterlin, A. *J. Appl. Phys.* 1969, **40**, 4238
31 Akaoku, R. J. and Peterlin, A. *J. Polym. Sci. A2* 1971, **9**, 895
32 Morsoff, N. and Peterlin, A. *J. Polym. Sci. A2* 1972, **10**, 1237
33 Balta-Calleja, F. J., Peterlin, A. and Crist, B. *J. Polym. Sci. A2* 1972, **10**, 1479
34 Balta-Calleja, F. J. and Peterlin, A. *Die Makromol. Chem.* 1971, **141**, 91
35 Hay, I. L. and Keller, A. *J. Mater. Sci.* 1967, **2**, 538
36 Petraccone, Y., Sanchez, I. C. and Stein, R. S. *J. Polym. Sci., Polym. Phys. Edn.* 1975, **13**, 1991